JOURNAL OF GEOPHYSICAL RESEARCH, VOL. 115, D00I15, doi:10.1029/2009JD012379, 2010

Modulations of the 27 day solar rotation signal in stratospheric ozone from Scanning Imaging Absorption Spectrometer for Atmospheric Cartography (SCIAMACHY) (2003–2008)

Sebastian Dikty,[1] Mark Weber,[1] Christian von Savigny,[1] Thiranan Sonkaew,[1] Alexei Rozanov,[1] and John P. Burrows[1]

Received 30 April 2009; revised 5 November 2009; accepted 17 November 2009; published 29 April 2010.

[1] Here we investigate the modulating nature of the 27 day solar rotation forcing on stratospheric ozone using a new ozone profile data set from Scanning Imaging Absorption Spectrometer for Atmospheric Cartography (SCIAMACHY, 2003–2008). Continuous wavelet transform (CWT), fast Fourier transform (FFT), and cross correlations (CC) have been applied to SCIAMACHY ozone in the tropics (<20° latitude) between 20 and 60 km altitude. The maximum correlation between Mg II index and ozone is weaker during the maximum of solar cycle 23 (r = 0.38) than in the previous two solar cycles that have been investigated in earlier studies using different data sets. The magnitude of the ozone signal is highly time dependent and may vanish for several solar rotations even close to solar maximum conditions. The FFT analysis reveals, besides the 27 day signal, several frequencies close to 27 days. The ozone sensitivity (ozone change in percent per percent change in 205 nm solar flux) is on average about 0.2%/% above 30 km altitude and smaller by about a factor of 2 compared to earlier studies. For selected 3 month periods the sensitivity may rise beyond 0.6%/% in better agreement with earlier studies. The analysis of the 27 day solar forcing was also carried out with stratospheric temperatures from European Centre for Medium-Range Weather Forecasts operational analysis. Although direct radiation effects on temperature are weak in the upper stratosphere, temperature signals with statistically significant periods in the 25–35 day range similar to ozone could be found with the applied methods.

Citation: Dikty, S., M. Weber, C. von Savigny, T. Sonkaew, A. Rozanov, and J. P. Burrows (2010), Modulations of the 27 day solar rotation signal in stratospheric ozone from Scanning Imaging Absorption Spectrometer for Atmospheric Cartography (SCIAMACHY) (2003–2008), *J. Geophys. Res.*, *115*, D00I15, doi:10.1029/2009JD012379.

1. Introduction

[2] The differential rotation of the Sun causes regions with intensified radiative output to appear and disappear within the field of view of the earth. Depending on the solar latitude the Sun's rotational period varies from 25 days near the equator to 35 days close to the poles [*Lean*, 1991]. The frequency and latitudinal distribution of the Sun spots and active regions also vary with the 11 year solar cycle and modulate the radiative output of the Sun. The solar variation on the 11 year time scale has been shown to cause 2–3% variability in tropical ozone at altitudes of approximately 40 km. This has been concluded from satellite observations [e.g., *Hood*, 2004; *Fioletov*, 2009; *Remsberg*, 2008; *Randel and Wu*, 2007; *Soukharev and Hood*, 2006] and confirmed by model studies [e.g., *Marsh et al.*, 2007; *Sekiyama et al.*, 2006; *Langematz et al.*, 2005]. In general, the models show a lower altitude for the maximum ozone sensitivity to solar forcing than observations. Differences between observations and model still remain for the lower stratosphere. *Fioletov* [2009] estimated from the 27 day ozone response the 11 year ozone response with the help of a statistical model. He also emphasized the fact that only three complete periods of the 11 year solar cycle were covered by satellite observations so far. In addition, the life span of a single satellite instrument is generally far less than one solar cycle and instrumental biases between different ozone profile data sets complicate statistical analysis of decadal variations.

[3] The influence of the 27 day solar rotation on ozone has already been investigated by *Hood* [1986] in the 1980s using SBUV (Solar Backscatter UltraViolet) ozone measurements during solar maximum of solar cycle 21 (1979–1981). He found the ozone sensitivity at 45 km to be slightly more than 0.4% per 1% change in the 205 nm flux. Further investigations with different satellite data sets and model outputs covering other time periods followed [e.g., *Hood and Zhou*, 1998; *Zhou et al.*, 2000; *Williams et al.*, 2001; *Rozanov et al.*, 2006; *Ruzmaikin et al.*, 2007; *Fioletov*, 2009]. Especially, *Fioletov* [2009] examined a time series of ozone

[1]Institute of Environmental Physics, University of Bremen, Bremen, Germany.

0148-0227/10/2009JD012379

measurements from various satellite instruments from the SBUV series from 1979 to 2006. Compared to the findings of *Hood* [1986] the ozone response is in good agreement (0.4%/%). *Austin et al.* [2007] and *Gruzdev et al.* [2009] compared the 27 day ozone variability determined by chemistry climate models (CCM) with satellite measurements and were able to verify the observations in magnitude (0.4 to 0.5%/%) but found the maximum ozone sensitivity slightly lower in altitude (~40 km) in the model simulations. A detailed summary of 27 day ozone variations from past observations is given by *Gruzdev et al.* [2009]. *Ruzmaikin et al.* [2007] used the empirical mode decomposition on Microwave Limb Sounder (MLS) ozone (2004 to 2006) to show the altitude/latitude distribution of the 27 day mode. He found the highest 27 day amplitude to be in the winter high latitudes of the upper stratosphere. The term "27 days" will be used throughout this paper to describe variations on time scales of 25 to 32 days that are likely related to solar rotational variations.

[4] The scope of this paper is to investigate short-term variations (approximately 27 days) in stratospheric ozone. Dominant frequencies may vary according to the section of the time series investigated. This makes it necessary to introduce new frequency analysis approaches, such as the continuous wavelet transform (CWT), in addition to the more traditional approaches. A second motivation is that a new ozone profile data set is available from SCIAMACHY that spans a large part of the recent solar cycle 23 and beginning of the current cycle and is well suited for studies on short-term solar variations.

[5] We use the fast Fourier transform (FFT) [*Bracewell*, 2000], cross correlations (CC) and the already mentioned CWT [*Torrence and Compo*, 1998] for our time series analysis of SCIAMACHY limb scatter ozone and European Centre for Medium-Range Weather Forecasts (ECMWF) temperature profiles. The SCIAMACHY data have a high spatial sampling with global coverage of the sunlit Earth achieved within 6 days, which makes this data set valuable for studying short-term variability in the middle to upper stratosphere. The CWT in particular has become more popular over the last 2 decades. While the FFT and CC are common tools in time series analysis, their main disadvantage is that the time series is treated as a whole and temporal fluctuations in the signal period cannot be detected. The CWT offers a higher temporal resolution with a combined adjustment between time and frequency resolution depending on the choice of wavelet and its order. Within a given time series the connection between ozone and solar radiation is sometimes not well-defined and this can be studied in a suitable way with CWT in combination with other frequency analysis tools.

[6] The FFT, CC, and CWT have been applied to both the tropical ozone profiles and the Mg II index, the latter being a common proxy for solar activity and irradiance changes. Both quantities were derived from SCIAMACHY observations [*Skupin et al.*, 2005; *von Savigny et al.*, 2005a; *Sonkaew et al.*, 2009]. In order to identify possible mechanisms for a solar rotation signal on stratospheric ozone, it is worthwhile to look at corresponding stratospheric temperature variations; for example, a recent study by *Ruzmaikin et al.* [2007] showed 27 day variations in stratospheric temperatures. *Gruzdev et al.* [2009, Figure 14, and references therein] nicely summarize earlier findings regarding the temperature sensitivity in the stratosphere observed by SAMS and MLS, and compare these findings with their 3D model output. Both, observations and model show sensitivities in the range of 0.02 to 0.04%/% in stratospheric temperatures. These results are in agreement with findings from *Brasseur et al.* [1987], who used a 1D model with a sinusoidal 27 day solar forcing and compared their results to SAMS observations reported by *Keating et al.* [1987]. The same frequency analyses FFT, CC and CWT were, therefore, also applied to stratospheric temperatures from ECMWF operational analyses during the SCIAMACHY observation period (2003–2008) to allow a better evaluation of the indirect effects of solar-ozone interactions and to identify possible links to temperature-dependent ozone chemistry. Variations in stratospheric temperatures, if correlated with corresponding ozone changes on such a short-term time scales, may also be indicators for dynamical responses to solar forcing in addition to chemical and radiative effects.

2. Data Sources

2.1. SCIAMACHY Ozone Data

[7] A comprehensive summary of the SCIAMACHY instrument is given by *Bovensmann et al.* [1999]. SCIAMACHY is one of 10 instruments on board the European satellite ENVISAT (European Environmental Satellite), which was launched in March 2002. ENVISAT is in a Sun-synchronous orbit with an inclination of 98.5°, a mean altitude of 796 km and has a period of 100 min thus performing about 14 to 15 orbits per day. The vertical resolution of the retrieved ozone profiles, as given by the full width at half maximum of the averaging kernels, is about 4.5 km, the vertical sampling approximately 3.3 km, and its instantaneous field of view 2.8 km. The limb spectra are measured in the flight direction of the satellite. The overall yield is roughly 10,000 profiles per month. Except for polar night regions, global coverage is achieved within 6 days. The time for tropical SCIAMACHY observations is close to 1000 local time.

[8] SCIAMACHY is an eight-channel spectrometer covering the spectral range from 240 nm to 2380 nm. It uses different viewing geometries for retrieving total trace gas columns (nadir) and profiles (limb and solar/lunar occultation) [*Bovensmann et al.*, 1999]. The limb retrieval uses wavelengths in the Hartley-Huggins (264, 267.5, 273.5, 283, 286, 288, 290, and 305 nm) and Chappuis (525, 600 and 675 nm) ozone absorption band and covers altitudes from 10 to 60 km. The multiple scattering radiative transfer model SCIATRAN 2.0 [*Rozanov et al.*, 2005] is used in the forward modeling as part of the optimal estimation inversion. The ozone profile data was retrieved on a vertical one km altitude grid, which provided more stable profile retrievals compared to a coarser resolution. A complete description of the ozone limb retrieval is given by *von Savigny et al.* [2005a] and *Sonkaew et al.* [2009]. The version 2.1 ozone profile data set derived from SCIAMACHY limb observations is used here. Earlier versions including only the Chappuis wavelengths in the retrieval [*von Savigny et al.*, 2005a], thus limiting retrieved altitudes up to 40 km, were in good agreement with HALOE and SAGE II (within 10%). However, earlier data suffered from a varying shift in the tangent height [*von Savigny et al.*, 2005b]. In the new

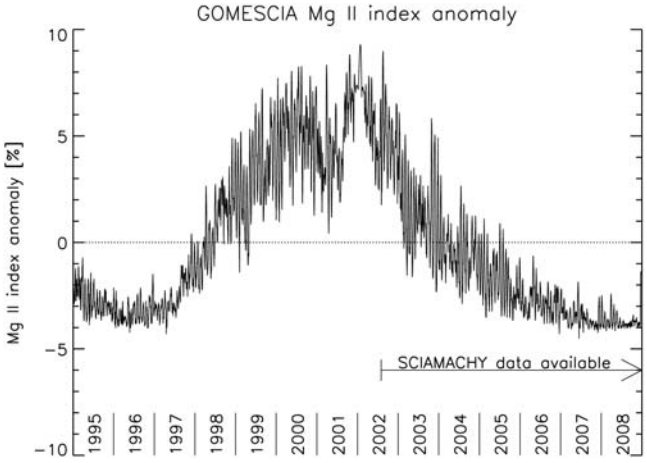

Figure 1. Composite Mg II index anomaly from GOME and SCIAMACHY solar observations from 1995 to 2008. The SCIAMACHY observation period covers the declining phase of solar cycle 23 from 2003 to 2008.

data version, the tangent height offset has been successfully corrected and agreement of the limb ozone profiles with other satellite data (HALOE and SAGE II) are now improved to better than 10% on average up to 50 km altitude (S. Mieruch et al., manuscript in preparation, 2010).

2.2. Solar Proxy: Mg II Index

[9] For the cross-correlation analysis a suitable proxy for solar UV irradiance variation is needed. *Hood* [1986] used the 205 nm irradiance as a solar proxy since molecular oxygen is primarily photodissociated at wavelengths between 183 and 205 nm in the upper stratosphere. The Mg II index is given by the core-to-wing ratio of the Mg II h and k doublet at 280 nm and was shown to correlate well with solar UV irradiance changes throughout the UV region down to 30 nm [*DeLand and Cebula*, 1993; *Weber*, 1999; *Viereck et al.*, 2004]. The Mg II absorption originates in the Sun's photosphere, while the narrow emission core stems from the chromosphere above. The chromospheric solar activity varies with temperature and surface magnetic activity and is, therefore, a good measure of solar UV irradiance variation. Since it is a ratio, it is insensitive to the optical degradation of the measuring instrument. A 1% change in the GOMESCIA Mg II index corresponds to a 0.61% change in the solar flux at 205 nm. In addition to atmospheric measurements, SCIAMACHY provides daily solar irradiance measurements from which a daily Mg II index can be derived [*Skupin et al.*, 2005]. This Mg II index has been combined with data from SBUV (1979–1992), SUSIM (1992–1995), and GOME (1995–2001) to obtain a composite Mg II index spanning nearly 3 decades [*Weber*, 1999; *Viereck et al.*, 2004]. The composite Mg II index, also called GOMESCIA Mg II index, from GOME and SCIAMACHY solar irradiance measurements from 1995 to 2008 (solar cycle 23) is shown in Figure 1. The 27 day solar rotational variations during solar maximum are almost half the magnitude of an entire 11 year solar cycle [*Weber*, 1999; *Skupin et al.*, 2005].

2.3. ECMWF Temperatures

[10] Stratospheric temperature data are taken from the ECMWF operational analysis available at 1.5° by 1.5° spatial resolution. The main source of data for ECMWF stratospheric temperatures are from the Advanced Microwave Sounding Unit-A (AMSU-A), the Atmospheric Infrared Sounder (AIS) and the High-Resolution Infrared Radiation Sounder (HIRS). Observational data up to approximately 50 km are being assimilated. Zonal mean data for the latitude band 20°S to 20°N were calculated from 20 to 60 km in steps of one km. Figure 2a shows the cross correlation between unfiltered stratospheric ozone and temperatures from 20 to 60 km. Ozone and temperature are highly anticorrelated above 35 km peaking at 40 km ($r < -0.85$) with approximately zero time lag, and highly correlated below 28 km peaking at 20 km ($r > 0.9$) with a time lag of approximately 20 days. The origin of the high absolute correlation comes mainly from the seasonal variation in stratospheric temperatures and ozone (concluded from the CC of seasonal fits to ECMWF

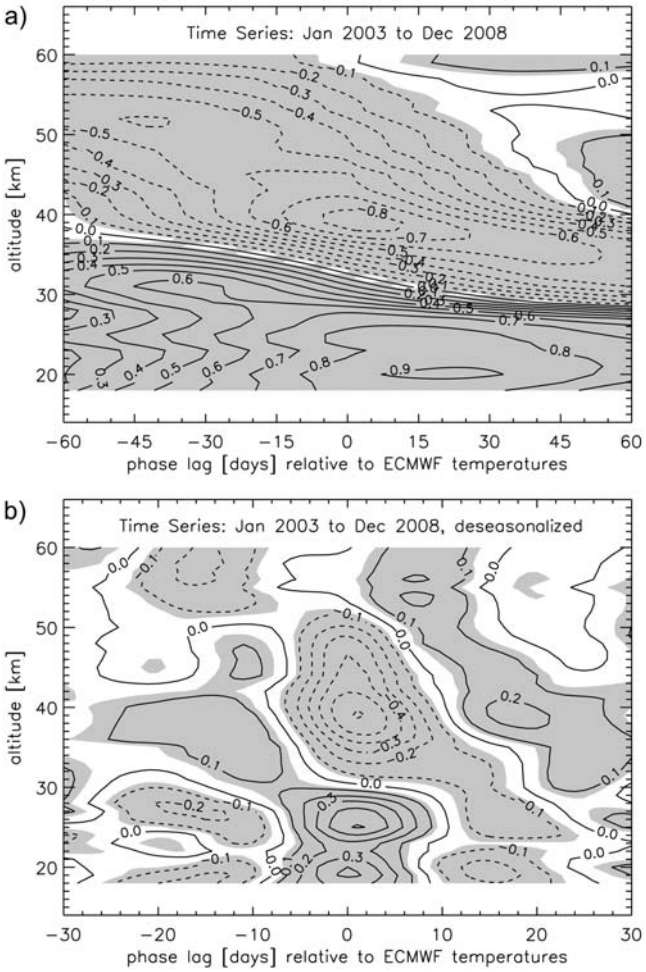

Figure 2. Cross correlation of tropical zonal mean SCIAMACHY ozone and ECMWF temperature anomalies (20°S–20°N) between 20 and 60 km (a) with the unfiltered time series and (b) after the seasonal cycle has been removed. The shading indicates statistical significance being greater than 95%.

temperatures and SCIAMACHY ozone showing a similar picture, but not shown here). Figure 2b now shows the cross correlation between the ozone and temperature with the seasonal cycle removed. Above 30 km anticorrelation is as low as −0.6 and below 30 km the correlations are up to 0.5, in both cases for zero time lag. The anticorrelation in the upper stratosphere is mainly caused by the negative temperature dependence of the ozone production ($O_2 + O + M \rightarrow O_3 + M$) in the Chapman reaction cycle, decreasing the O/O_3 ratio with decreasing temperature [*Rosenfield et al.*, 2002]. In the lower stratosphere the lifetime of ozone is longer, atmospheric transport and the catalytic ozone loss cycles play a larger role. In addition to the impact on ozone production, the ozone loss ($O + O_3 \rightarrow 2O_2$) is significantly slowed down with decreasing temperature [*Sander et al.*, 2005; *World Meteorological Organization*, 2007].

3. Data Analysis

3.1. Ozone Data Preprocessing

[11] All profiles between 20°S to 20°N latitude for a given day were selected and an area-weighted zonal mean profile was calculated. Days with less than ten profiles within this latitude band were treated as days with no data. Daily zonal mean SCIAMACHY ozone profiles were derived from 20 km to 60 km altitude in steps of one km. Ozone anomalies were calculated by subtracting the long-term mean from 2003 to 2008. Major outliers in the time series are identified as being outside the 3σ value from the zonal mean at each altitude and are rejected. Anomalies in ozone as well as temperature from January 2003 to December 2008 are illustrated for the 20–60 km altitude range in Figure 3. Annual variations in ozone are dominant above 40 km and a QBO (Quasi Biennial Oscillation) signal can be identified below [*Huang et al.*, 2008; *McCormack et al.*, 2007].

[12] Filtering of the time series becomes necessary to separate known frequencies from a potential 27 day signal. Otherwise these frequencies may dominate the time series. The first filter is the subtraction of a 6 day running mean (smoothing) to eliminate fluctuations on very short time scales (Figure 3). Six days were chosen because SCIAMACHY fully covers the Earth in 6 days and contributions from all longitudes were desired. Choosing an even number of days for the running mean shifted the time series by half a day. This shift has also been applied to the solar proxy and ECMWF temperatures. Before the 6 day running mean was applied, data gaps were closed using a spline interpolation. Data gaps normally occur due to maintenance operations on the instrument or satellite platform and rarely last more than a few days. In case of the larger data gap between 29 January and 23 February 2005, the spline interpolation introduced an artifact in such a way that the amplitude is overestimated in the frequency analysis. The 6 day running mean was applied to all time series used in this study before any other filter or analysis method was applied.

3.2. Fast Fourier Transform

[13] A FFT was applied to the unfiltered SCIAMACHY ozone and ECMWF temperature anomalies. The resulting power spectrum can be seen in Figure 4. Similar results are obtained if the semiannual, annual, and QBO terms from a multivariate least squares approach are subtracted from the time series before FFT application (not shown here). For ozone, a peak at 26 and 28 days at altitudes of approximately 35 km and above 45 km are visible. In addition, the first harmonics, the 13.5 days signal, is visible at approximately 35 km. Whether or not any high-pass filter or the 6 day smoothing (low-pass filter) was applied to the time series before does not change the result of the FFT. It can also be seen in Figure 4 that the 27 day ozone signal is in fact a collection of periods ranging from 25 to 32 days for the 2003 to 2008 ozone data. As for temperature, peaks are visible at 29 days at altitudes of approximately 35 and 50 km, and also a peak at 23 days at an altitude of approximately 45 km. The overall magnitude of the temperature signal is by more than 1 order of magnitude less than compared to the ozone signal, which is due to the smaller amplitude of temperature variations.

3.3. Cross Correlation

[14] For comparisons to studies by *Hood* [1986], *Fleming et al.* [1995] and *Hood and Zhou* [1998] a cross-correlation analysis was performed on SCIAMACHY ozone and ECMWF temperatures. A 35 day running mean was subtracted from the unfiltered time series to remove variations on large time scales, e.g., the (semi)annual and the QBO signal. An example of the 35 day filtered final time series is shown in Figure 5, where a periodic signal with a period of approximately a month is detectable for ozone and temperature at 45 km altitude.

[15] Mg II index and ozone anomaly time series from SCIAMACHY at selected altitudes are shown in Figure 6. It is evident that both time series track each other nicely for some brief periods; at other times, however, the correlation vanishes as highlighted in Figure 7. The correlation strongly depends on the examined period.

[16] Cross correlations with time lags between ozone (Figures 8a, top, through 8c, top) and temperature (Figures 8a, bottom, through 8c, bottom) and the Mg II index as a function of altitude are shown for different time segments: the entire observation period (2003 to 2008) (Figure 8a), close to solar maximum (2003 to 2004) (Figure 8b), and at solar minimum (2006 to 2007) (Figure 8c). The 27 day signal is statistically significant near solar maximum and considerably weakens near solar minimum. However, from Figure 7 it is also clear that during some periods close to solar maximum the solar signal in ozone may vanish. Close to solar maximum, the maximum correlation in ozone is 0.38 with a phase lag of approximately 3 days (no phase lag below 35 km). The overall structure of the ozone CC is in agreement with work by *Hood* [1986] and *Hood and Zhou* [1998]; however, the correlation is lower than during maxima of solar cycle 21 (1979 to 1980) and solar cycle 22 (1990 to 1991) as reported by *Hood* [1986] and *Hood and Zhou* [1998], and there is a phase shift of the maximum correlation with altitude by about 5 days between 30 and 45 km, which is not visible in the SCIAMACHY analysis. As for temperature, near solar maximum correlations are weak, yet significant, and increasing above 50 km. During solar minimum the correlation weakens and below 30 km an anticorrelation is visible with approximately 2–3 days time lag.

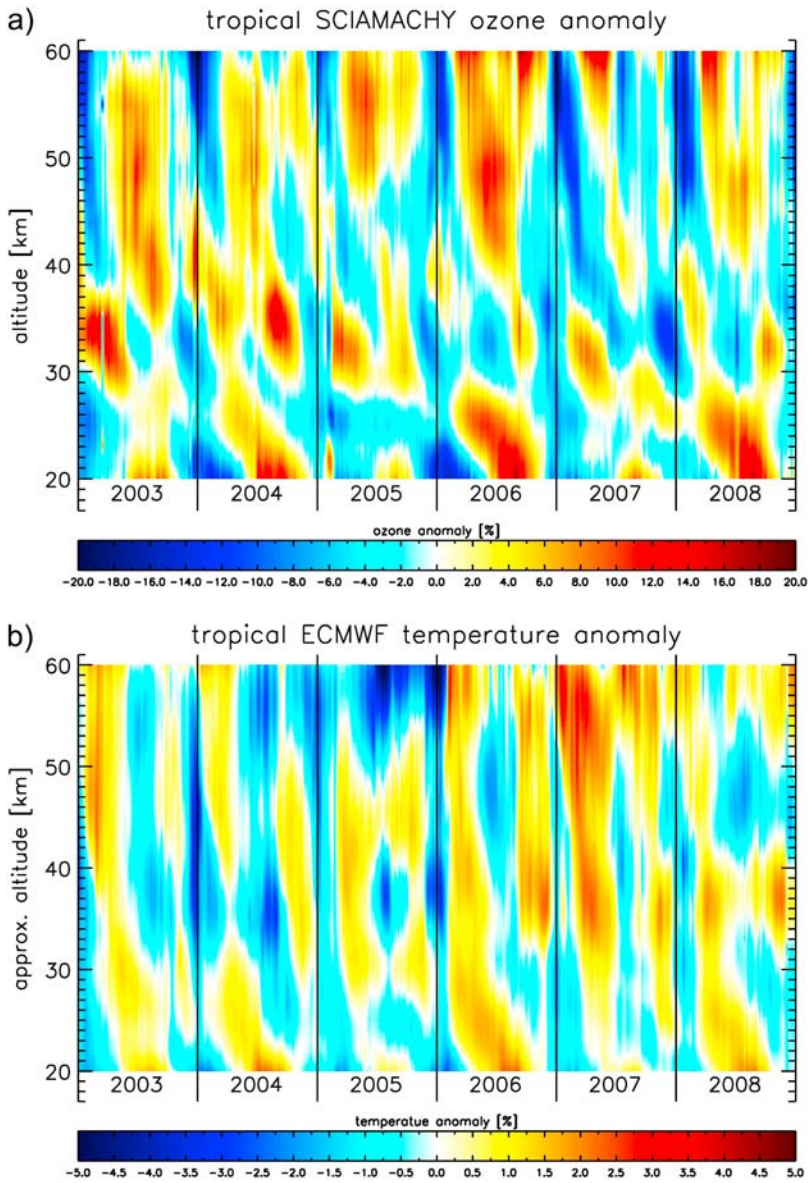

Figure 3. Zonal mean anomaly of (a) SCIAMACHY ozone and (b) ECMWF temperature (20°S–20°N) between 20 and 60 km altitude from 2003 to 2008.

3.4. Wavelet Analysis

[17] As shown in Figure 7, the correlation between the 27 day solar signal and ozone varies strongly with time. A CWT has the advantage of showing frequencies contained in a time series as a function of time. The Morlet wavelet with an order of 24 was chosen for the transform [*Percival and Walden*, 2006]. This choice provides a good compromise between frequency resolution and time resolution in the power spectrum.

[18] Discontinuities at both ends of the power spectra occur due to the finite nature of our time series. The so called "cone of influence" is therefore limited to the inner part of the spectrum bordered by the dashed lines in Figures 9 and 10. Solid contour lines denote the 99% confidence level, which was calculated by testing the wavelet spectra against a theoretical background wavelet spectrum (red or white noise) [*Torrence and Compo*, 1998]. The lower the frequencies the more of the wings of the spectrum can be regarded as statistically insignificant. The Morlet wavelet was also applied to the extended SCIAGOME Mg II index going back to 1979 [*Weber*, 1999] as shown in Figure 9a. The power spectrum as well as the Mg II index itself clearly shows the increased 27 day amplitude of the Mg II index during solar maximum. The 27 day as well as its first harmonics, the 13.5 day peak, can be identified. Apart from the stronger 27 day signal during solar maximum, it is also evident that solar cycles 21 and 22 were more intense than solar cycle 23 regarding the 27 day signal during solar maximum, especially solar cycle 22 with relative anomaly amplitudes of up to 5%, which is more than half of the amplitude between solar maximum and solar minimum (11 year cycle). Figure 9a also indicates that the disk averaged solar rotation has varying periods ranging

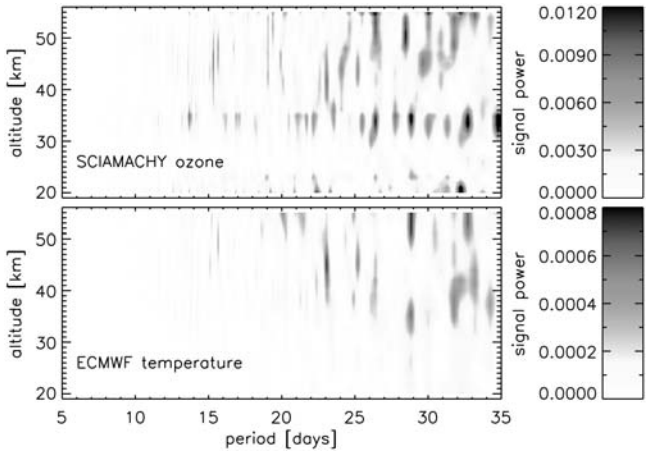

Figure 4. FFT power spectrum of zonal mean (top) SCIAMACHY ozone and (bottom) ECMWF temperature anomalies (20°S–20°N) from 2003 to 2008 between 20 and 55 km.

from 25 to 32 days. *Ebel et al.* [1981] noted 25 day periodic response in temperature and geopotential height at 50, 30 and 10 hPa from solar forcing. The second harmonics, a 9 day signature as identified in the SBUV ozone time series [*Fioletov*, 2009], is not visible in the CWT of the Mg II index. Only the 27 day signal is above the 99% level of confidence, which is marked by solid lines in Figure 9a.

[19] For a better comparison with SCIAMACHY ozone data, this CWT analysis of the Mg II index has been repeated for the shorter SCIAMACHY observation period from 2003 to 2008 as shown in Figure 9b. This time the 35 day running mean has already been subtracted to remove low frequencies and to treat the Mg II index in the same way as the ozone and temperature data. Again, the 27 day and 13.5 day peaks are clearly visible. The corresponding CWT for ozone and temperature is shown in Figure 10 for altitudes of 30, 45 and 55 km.

[20] The power spectrum of SCIAMACHY ozone shows a peak at approximately 25 days, but limited to altitudes between 42 and 47 km (see Figure 10c for 45 km). This is a slightly higher frequency than the mean solar signal input (27 days). Below this altitude the signal power becomes rather faint lacking a clear peak (Figure 10a). Above 47 km the power spectra show stronger signals, but with broader peaks covering frequencies between 23 and 32 days in selected years (Figure 10e, 2004 and 2006–2007). In the first half of 2005, strong peaks are visible, not only in the ozone time series but also in the power spectrum. Due to a change in SCIAMACHY mission operations, tropical ozone data were not available from 29 January 2005 to 23 February 2005 (marked with dashed vertical lines in Figure 10) causing fake signals in the CWT and therefore has to be treated with caution. Especially in Figure 10a, a fake signal is visible in early 2005. Apart from this signal, the CWT of SCIAMACHY ozone at 30 km reveals weak and mostly statistically insignificant signals inside the cone of influence.

[21] The CWT for ECMWF temperatures shows smaller signal strengths compared to ozone, which again is due to its smaller amplitude. Nevertheless, these signals are statistically significant. At 30 km a 30 day peak for early 2008 and a 35 day peak for 2004 are visible. The CWT for 45 km reveals a peak structure going from 23 days up to 35 days from late 2004 to late 2006 similar to ozone. Above that height at 55 km the signals become stronger, with peaks in late 2004 (23–35 days), and in early 2006 (20 days and 28–30 days). Both ozone and temperature CWT show similar time-varying frequency signals in the period range of 25 to 35 days throughout the SCIAMACHY observation period, while CWT of the Mg II index shows marked signals only close to 27 days and during solar maximum. This may suggest that periodic variations in the temperature and ozone in the time scale of 25 to 35 day periods may not only be

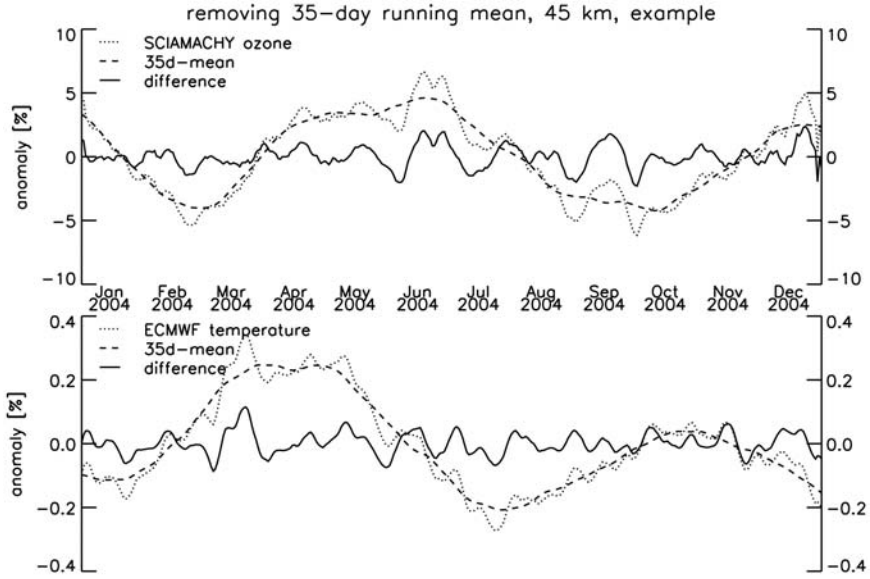

Figure 5. Example of (top) SCIAMACHY ozone and (bottom) ECMWF temperature anomaly time series at 45 km altitude in year 2004 before and after subtracting a 35 day running mean.

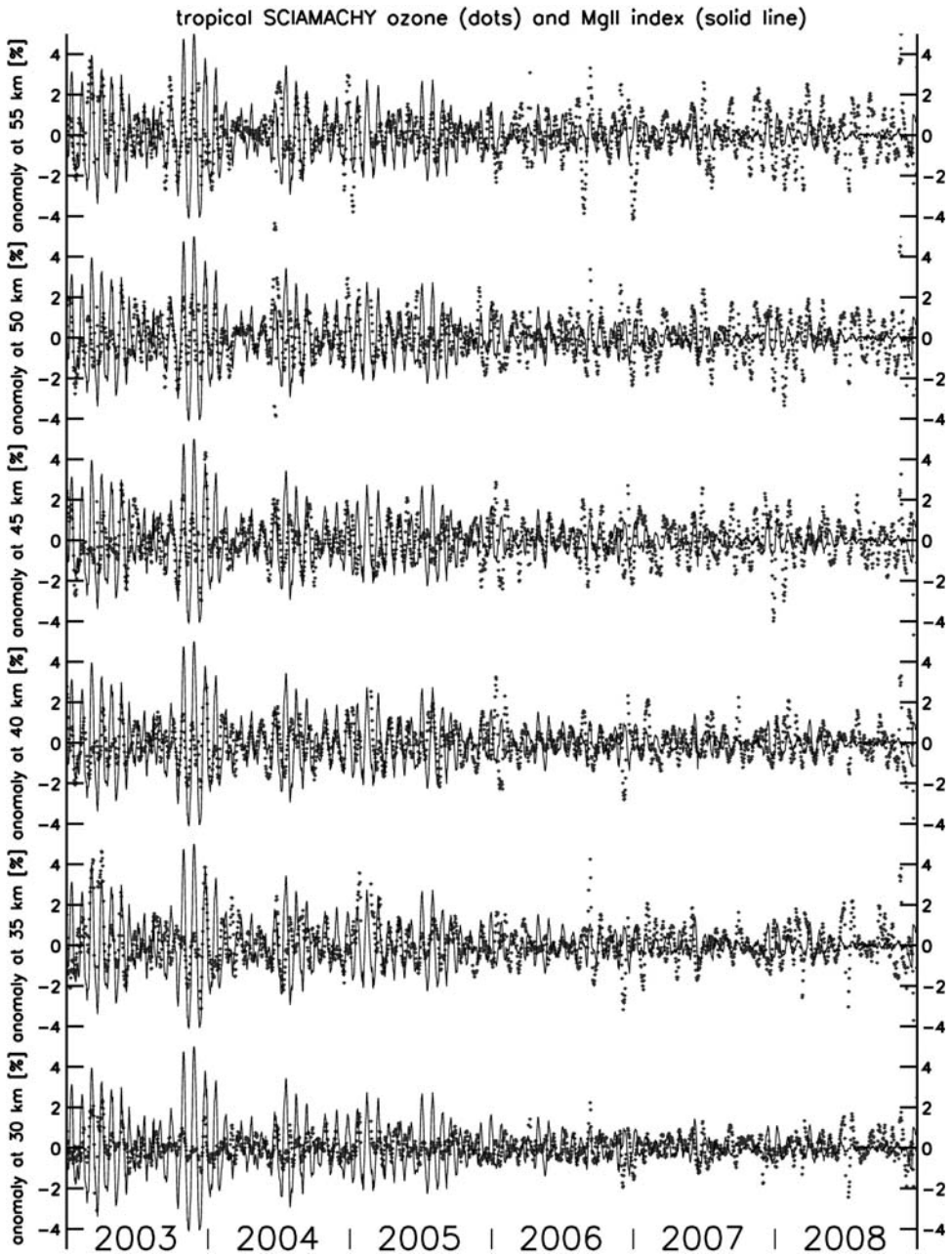

Figure 6. SCIAMACHY zonal mean ozone anomaly (20°S–20°N) (solid line) and Mg II index anomaly (solid circles) in percent at selected altitudes (from top to bottom: 55, 50, 45, 40, 35 and 30 km). A 35 day running mean was removed in all time series.

due to solar variability. An exception is the broad frequency signal in the Mg II CWT at the end of 2003 (25–32 days), which shows a corresponding pattern in ozone only at 45 km altitude, but not in temperature.

3.5. Ozone Sensitivity to 27 Day Solar Radiation Changes

[22] The altitude-dependent sensitivity of tropical SCIAMACHY ozone to variations in the 205 nm solar irradiance flux (converted from Mg II index as explained in section 2.2) is shown in Figure 11. The solid line indicates the mean sensitivity from the correlation method and dashed lines denote the 2σ uncertainty. The ozone sensitivity is plotted for the complete time series (Figure 11, left, 2003–2008), conditions close to solar maximum (Figure 11, middle, 2003–2004), and solar minimum (Figure 11, right, 2006–2007). Comparisons with model results from Figure 10 of *Gruzdev et al.* [2009] and observational data results from Figure 4 of *Fioletov* [2009] show differences in the altitude of maximum sensitivity. Their ozone sensitivity peaks near 40 km for the observations and slightly below for model output, while the peak for SCIAMACHY is at approximately 35 km, and a second but smaller one at 43 km close to solar maximum conditions. The amplitude of the observed ozone sensitivity is a factor of 2–3 smaller than summarized by *Gruzdev et al.* [2009]. From Figure 7 it

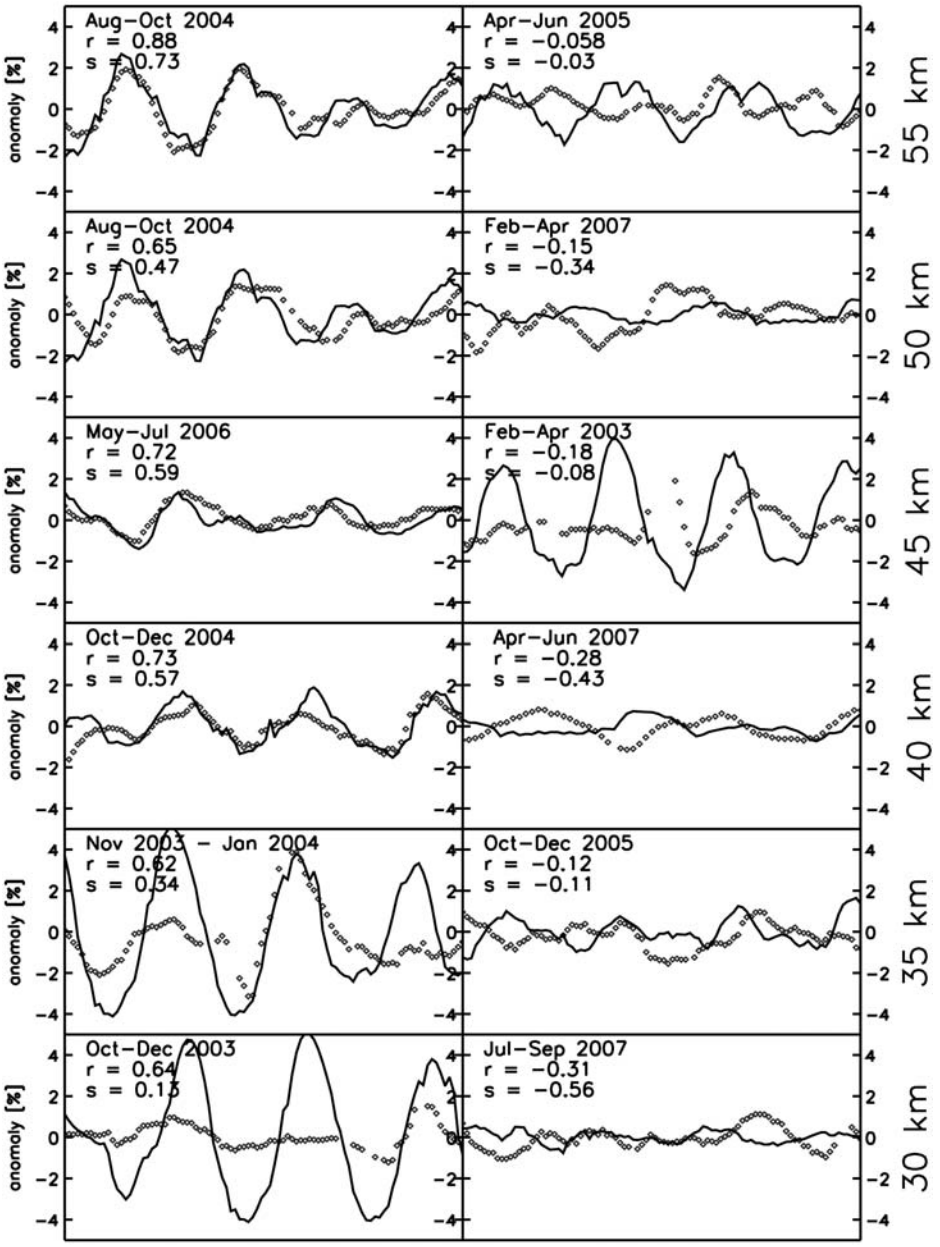

Figure 7. Selected 3 month periods from Figure 6 with (left) high and (right) low correlation between ozone (solid line) and Mg II index (circles). In each plot the period, correlation (r), and ozone sensitivity (s), the latter being defined as ozone change per Mg II index change in units of %/%, are indicated. The ozone sensitivity per unit 205 nm solar irradiance change is obtained by multiplying s with 0.61.

can be shown that for some three month periods, e.g., August–October 2004, SCIAMACHY ozone sensitivity is in better agreement with work by *Gruzdev et al.* [2009] and *Fioletov* [2009].

4. Discussion

[23] The CC between the Mg II index and SCIAMACHY ozone and between Mg II index and ECMWF temperature for heights between 20 km and 60 km are summarized in Figure 8. The results for ozone are similar to the findings from *Hood* [1986] and *Hood and Zhou* [1998]; however, the absolute value for the maximum correlation is weaker. The maximum correlation in this study is 0.25 for the whole SCIAMACHY observation period (2003 to 2008). Close to solar maximum 23 in 2003 to 2004, the maximum correlation increases to 0.38, which is still considerably smaller than the model results from *Austin et al.* [2007] ($r > 0.8$) for this solar maximum and about 0.5–0.6 from earlier studies [*Hood*, 1986; *Hood and Zhou*, 1998]. The statistical significance is above the 2σ level as indicated by the gray shading in Figure 8. Limiting data to solar minimum conditions (2006 to 2007) considerably weakens correlations below statistical significance for most altitudes as can be seen in Figure 8c. *Hood* [1986] chose SBUV data from well within the solar maximum 21 (1979–1980), and also *Hood*

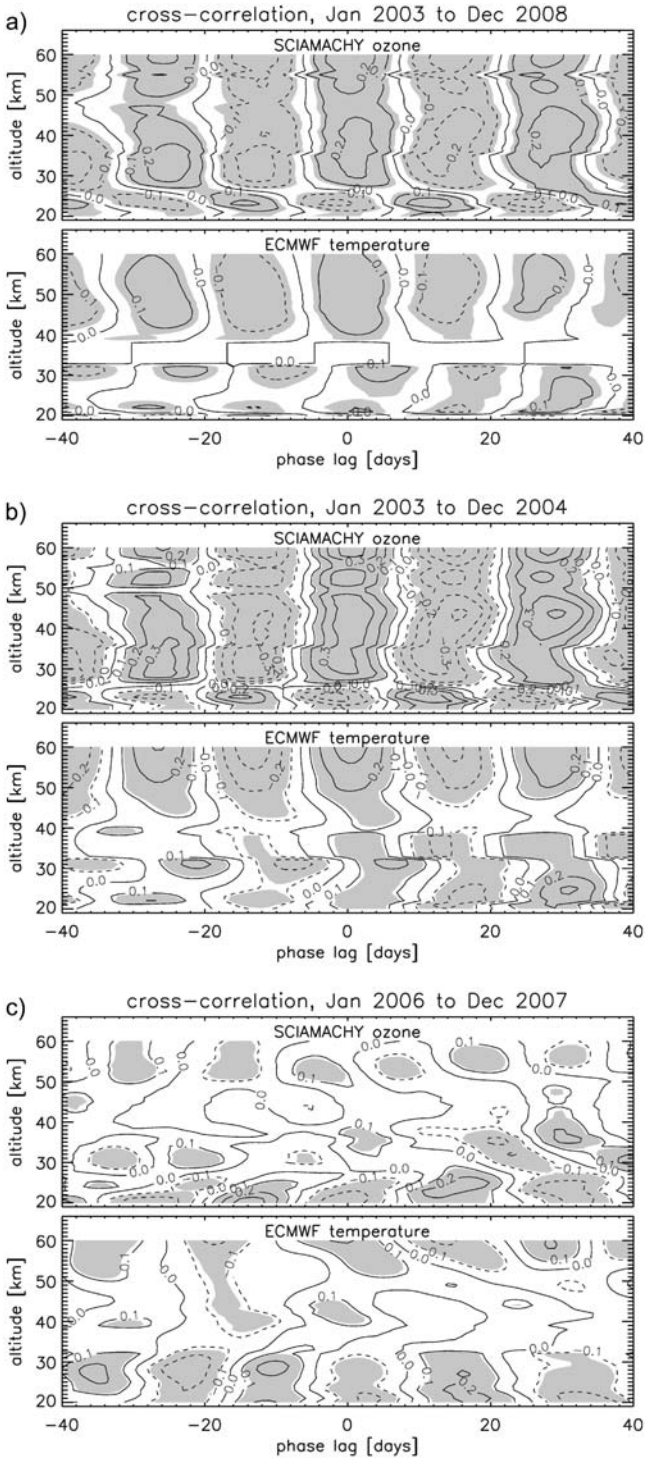

Figure 8. (a) Cross correlation of (top) SCIAMACHY ozone and (bottom) ECMWF temperature with Mg II index for the complete observation period (2003–2008). Shaded areas represent regions of statistical significance (2σ). (b) Same as Figure 8a but under solar maximum condition (2003–2004). (c) Same as Figure 8a but during solar minimum conditions (2006–2007).

and Zhou [1998] used MLS data from within solar maximum 22 (1990–1991). The first SCIAMACHY data were available from August 2002 onward, already on the declining branch of solar cycle 23 with smaller amplitudes in the 27 day variations, which we assume to be the reason for the difference of our ozone CC results to previous studies. Comparing our results from the CC to the results from model calculations done by Figure 2 of *Gruzdev et al.* [2009] reveals an agreement between the SCIAMACHY CC under solar maximum conditions and the model CC with solar forcing. However, the varying phase shift with altitude is not visible in the SCIAMACHY CC. The solar forcing in the model being shut off, the CC now rather compares well to the SCIAMACHY CC during solar minimum.

[24] *Ruzmaikin et al.* [2007] used the empirical mode decomposition (EMD) to investigate the 27 day solar variations in stratospheric ozone and temperature. They came to the same conclusions as we do about the general connection between ozone and temperature (Figure 2). They emphasized

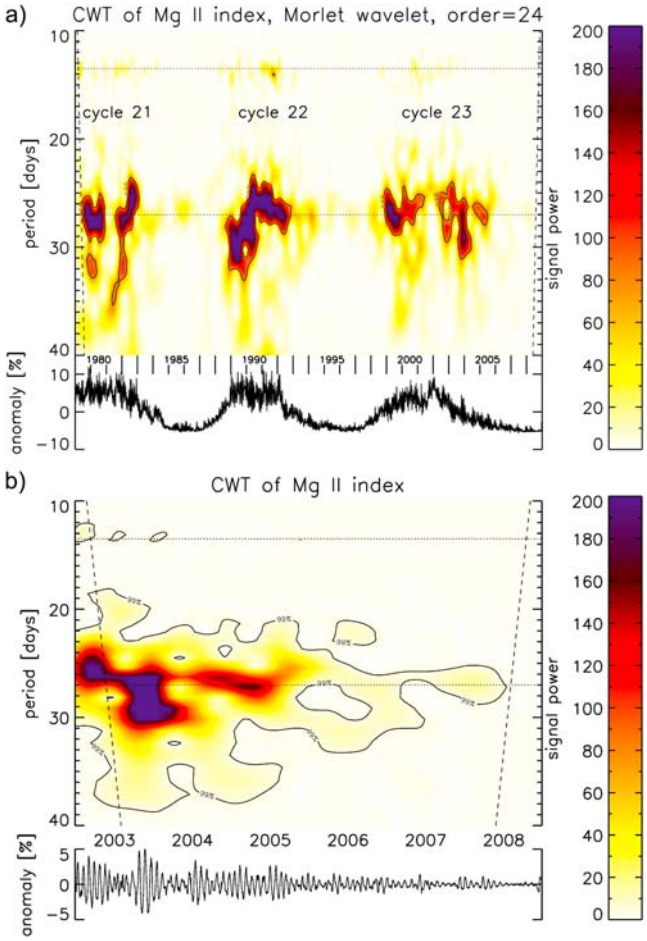

Figure 9. (a) Wavelet power spectrum as a result of the CWT applied to the composite Mg II index from 1979 to 2008. Peaks around 27 days as well as first harmonics, 13.5 days, are visible. The cone of influence is marked with dashed lines on either side. (b) Same as Figure 9a but with CWT only applied to Mg II data from the SCIAMACHY observation period. Solid contour lines indicate 99% confidence level.

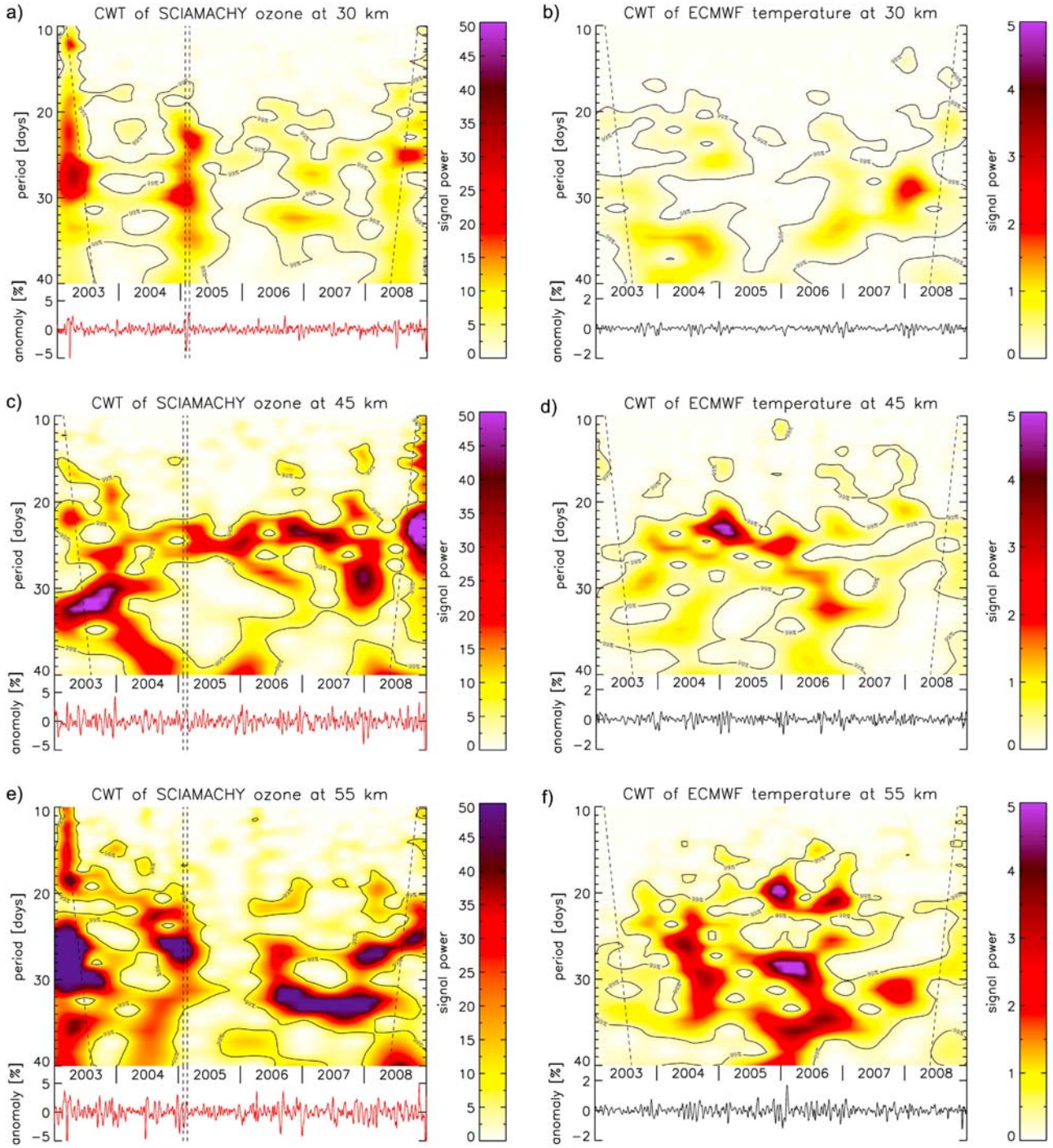

Figure 10. Wavelet power spectra at (a, b) 30 km, (c, d) 45 km, and (e, f) 55 km altitude, as a result of the CWT applied to (SCIAMACHY zonal mean ozone anomaly (20°S–20°N) (Figures 10a, 10c, and 10e) and ECMWF temperature (Figures 10b, 10d, and 10f). The temperature signal is about 1 order of magnitude weaker. Solid contour lines indicate 99% confidence level. The vertical dashed lines in Figures 10a, 10b, and 10e indicate the data gap in early 2005.

that interpreting any obvious correlations should be done with care since not only ozone but also temperature is dependent on UV changes. In the upper stratosphere the Chapman chemistry governs mainly ozone changes and this is also the region where we find the highest influence of UV radiation on ozone in our results. On the other hand, the influence of short-term variation in solar UV radiation on temperature in the upper stratosphere is weaker than it is on ozone (Figure 8). The influence becomes stronger above 50 km and below 30 km. According to *Ruzmaikin et al.* [2007] the tropical lower stratospheric vertical winds also show a 27 day signal, probably caused by wave disturbances

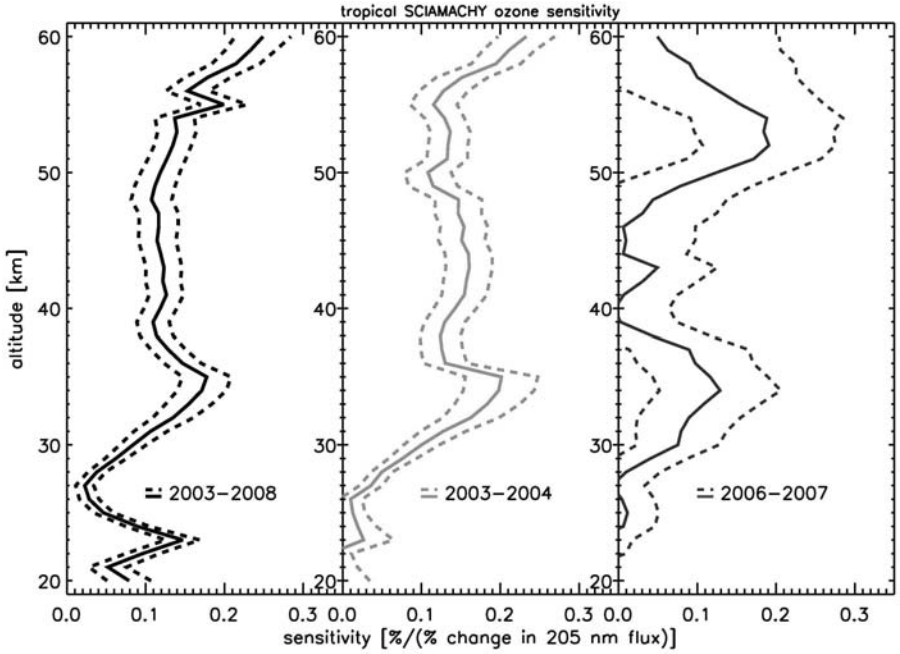

Figure 11. Altitude-dependent sensitivity of high-pass filtered tropical SCIAMACHY ozone (20°S–20°N) to variations in the 205 nm solar irradiance flux in units of %/%. Solid lines indicate the mean, and dashed lines denote the 2σ uncertainty. The sensitivity is plotted for (left) the complete time series (2003–2008), (middle) solar maximum (2003–2004), and (right) solar minimum (2006–2007).

or upwelling. In addition, they identified a 27 day solar UV signature in lower stratospheric tropical MLS (v1.51) temperature data.

[25] The CWT of the Mg II index (Figure 9a) shows that the amplitudes of the 27 day solar forcing are higher during solar maxima of solar cycle 21 and 22 than in solar cycle 23. Our results are consistent with findings from *Fioletov* [2009], who in addition showed that the 27 day solar forcing amplitude is weaker during solar minimum. He separated SBUV ozone data for all solar cycles (21 to 23) into solar maximum and solar minimum conditions (5 year intervals) and found that the ozone response to the 27 day solar forcing is not much different, whether it is solar maximum or minimum, although the 27 day signal in ozone goes below the 2σ level of significance during solar minimum. We were able to confirm this result with the CWT except that during solar minimum the significance does not even drop below the 3σ level (Figure 10c) and the periods are closer to 25 days. The most interesting result from our CWT analysis of SCIAMACHY ozone is the time-varying solar signal, bearing a collection of frequencies close to 27 days, which has been predicted by model simulations by *Rozanov et al.* [2006] and *Gruzdev et al.* [2009]. We also found the same collection of frequencies in the CWT of ECMWF temperature partially with the same signals in the CWT as for ozone implying the connection between ozone and temperature on short-term time scales. However, comparing the CWT power spectra of temperature to the power spectrum of the Mg II index does not reveal many similarities. The CC of temperatures with the Mg II index in the upper stratosphere show weaker correlations than for ozone. The broad frequency response (25–35 days) seen in both ozone and temperature CWTs throughout the SCIAMACHY observation period (Figure 10), but not evident in the Mg II index strongly suggest that apart from direct radiative effects, indirect effects from chemistry and/or atmospheric dynamics are important. This is in agreement with findings from *Brasseur et al.* [1987] and *Gruzdev et al.* [2009]. Other dynamical and chemical processes not related to solar activity cannot be ruled out to play a role as well here. A similarity in ozone at 45 km and Mg II frequency response appears to be only evident at the end of 2003 with strong periodic signals in the range of 25 to 32 days. During the Halloween 2003 solar storm unusually large variations in the solar radiation flux were measured by SCIAMACHY [*Pagaran et al.*, 2009].

[26] One has to carefully look at the selected part of the time series that is being investigated. Periodic signals in ozone vary with time and even vanish for several solar rotations independent of the phase of the larger 11 year solar cycle where the period was selected from. This large variability in solar response may be explained by other competing processes like atmospheric transport (dynamics) or chemistry (other than direct photochemistry), which become more important in the lower stratosphere [e.g., *Williams et al.*, 2001]. It cannot be ruled out that the latter mechanism may as well be triggered by short-term variations in solar forcing in the upper stratosphere, but are considered indirect effects.

5. Summary

[27] In this study we have used different approaches to analyze the relationship between the 27 day solar variations and stratospheric ozone. We also investigated the influence of the 27 day solar variations on ECMWF temperatures.

Some of the techniques were used to prove that SCIAMACHY ozone data are capable of confirming qualitatively results from earlier studies. Correlations are generally higher during solar maximum conditions, but even under solar maximum conditions correlations diminish for several solar rotations as discussed in sections 3.3 and 3.4.

[28] A wavelet analysis was used for the first time on satellite observations to investigate Sun-ozone interaction and allowed us to study the time-varying frequency content of the ozone, temperature, and Mg II index time series. Applied to the ozone time series, only altitudes close to 45 km show a clear 27 day signal. This is slightly above the height of maximum ozone sensitivity from earlier observations (40 to 45 km, depending on the study) and model runs (approx. 39 km) as summarized by *Gruzdev et al.* [2009]. However, ozone sensitivity to solar flux changes at 205 nm (most important for ozone production) is only half of that from other studies [*Gruzdev et al.*, 2009; *Fioletov*, 2009]. The same techniques as applied to SCIAMACHY ozone were used on the tropical zonal mean ECMWF temperature record between 2003 and 2008. Statistically significant time-varying signals in the power spectra of the temperature CWT were found for periods between 25 and 35 days throughout the SCIAMACHY observation period, and qualitatively agree with the ozone CWT. The CWT of Mg II index shows mostly strong signals very close to 27 days except at the end of 2003, where periodic signals from 25 to 32 days are observed in agreement with ozone (but not temperature) at 45 km altitude. The temperature CC shows weak but significant correlations around zero time lag. This suggests an indirect mechanism or even non-solar-related processes to play a more important role on these time scales, in particular for stratospheric temperature.

[29] **Acknowledgments.** We thank the DFG (Deutsche Forschungsgemeinschaft) for funding this study (SOLOZON project) as part of the German priority program CAWSES (Climate and Weather System of the Earth System). ECMWF temperature data were made available via the ECMWF special project SPDECDIO. We would also like to thank the unknown reviewers for their persistent help in improving this paper.

References

Austin, J., L. L. Hood, and B. E. Soukharev (2007), Solar cycle variations of stratospheric ozone and temperature in simulations of a coupled chemistry-climate model, *Atmos. Chem. Phys.*, *6*, 12,121–12,153.

Bovensmann, H., J. P. Burrows, M. Buchwitz, J. Frerick, S. Noël, V. V. Rozanov, K. V. Chance, and A. P. H. Goede (1999), SCIAMACHY: Mission objectives and measurement modes, *J. Atmos. Sci.*, *56*, 127–150.

Bracewell, R. N. (2000), *The Fourier Transform and its Applications*, McGraw-Hill, New York.

Brasseur, G., A. D. Rudder, G. M. Keating, and M. C. Pitts (1987), Response of middle atmosphere to short-term solar ultraviolet variations: 2. Theory, *J. Geophys. Res.*, *92*(D1), 903–914.

DeLand, M. T., and R. P. Cebula (1993), Composite Mg II Solar Activity Index for solar cycles 21 and 22, *J. Geophys. Res.*, *98*(D7), 12,809–12,823.

Ebel, A., B. Schwister, and K. Labitzke (1981), Planetary waves and solar activity in the stratosphere between 50 and 10 mbar, *J. Geophys. Res.*, *86* (C10), 9729–9738.

Fioletov, V. E. (2009), Estimating the 27-day and 11-year solar cycle variations in tropical upper stratospheric ozone, *J. Geophys. Res.*, *114*, D02302, doi:10.1029/2008JD010499.

Fleming, E. L., S. Chandra, C. H. Jackman, D. B. Considine, and A. R. Douglass (1995), The middle atmospheric response to short and long term solar UV variations: Analysis of observations and 2D model results, *J. Atmos. Terr. Phys.*, *57*(4), 333–365.

Gruzdev, A. N., H. Schmidt, and G. P. Brasseur (2009), The effect of the solar rotational irradiance variation on the middle and upper atmosphere calculated by a three-dimensional chemistry-climate model, *Atmos. Chem. Phys.*, *8*, 1113–1158.

Hood, L. L. (1986), Coupled stratospheric ozone and temperature response to short-term changes in solar ultraviolet flux: An analysis of Nimbus 7 SBUV and SAMS data, *J. Geophys. Res.*, *91*(D4), 5264–5276.

Hood, L. L. (2004), Effects of solar UV variability on the stratosphere, in *Solar Variability and Its Effects on Climate*, *Geophys. Monogr. Ser.*, vol. 141, edited by J. M. Papp and P. Fox, pp. 283–303, AGU, Washington, D. C.

Hood, L. L., and S. Zhou (1998), Stratospheric effects of 27-day solar ultraviolet variations: An analysis of UARS MLS ozone and temperature data, *J. Geophys. Res.*, *103*(D3), 3629–3638.

Huang, F. T., H. G. Mayr, C. A. Reber, J. M. Russel III, M. G. Mlynczak, and J. G. Mengel (2008), Ozone quasi-biennial oscillations (QBO), semiannual oscillations (SAO), and correlations with temperature in the mesosphere, lower thermosphere, and stratosphere, based on measurements from SABER on TIMED and MLS on UARS, *J. Geophys. Res.*, *113*, A01316, doi:10.1029/2007JA012634.

Keating, G. M., M. C. Pitts, G. Brasseur, and A. D. Rudder (1987), Response of middle atmosphere to short-term solar ultraviolet variations: 1. Observations, *J. Geophys. Res.*, *92*(D1), 889–902.

Langematz, U., J. L. Grenfell, K. Matthes, P. Mieth, M. Kunze, B. Steil, and C. Brühl (2005), Chemical effects in 11-year solar cycle simulations with the Freie Universität Berlin Middle Atmospheric Model with online chemistry (FUB-CMAM-CHEM), *Geophys. Res. Lett.*, *32*, L13803, doi:10.1029/2005GL022686.

Lean, U. (1991), Variations in the Sun's radiative output, *Rev. Geophys.*, *29*(4), 505–535.

Marsh, D. R., R. R. Garcia, D. E. Kinnison, B. A. Boville, F. Sassi, S. C. Solomon, and K. Matthes (2007), Modeling the whole atmosphere response to solar cycle changes in radiative and geomagnetic forcing, *J. Geophys. Res.*, *112*, D23306, doi:10.1029/2006JD008306.

McCormack, J. P., D. E. Siskind, and L. L. Hood (2007), Solar-QBO interaction and its impact on stratospheric ozone in a zonally averaged photochemical transport model of the middle atmosphere, *J. Geophys. Res.*, *112*, D16109, doi:10.1029/2006JD008369.

Pagaran, J. A., M. Weber, and J. P. Burrows (2009), Solar variability from 240 to 1750 nm in terms of faculae brightening and sunspot darkening from sciamachy, *Astrophys. J.*, *700*, 1884–1895.

Percival, D. B., and A. T. Walden (2006), *Wavelet Methods for Time Series Analysis*, Cambridge Univ. Press, Cambridge, U. K.

Randel, W. J., and F. Wu (2007), A stratospheric ozone profile data set for 1979–2005: Variability, trends, and comparisons with column ozone data, *J. Geophys. Res.*, *112*, D06313, doi:10.1029/2006JD007339.

Remsberg, E. E. (2008), On the response of Halogen Occultation Experiment (HALOE) stratospheric ozone and temperature to the 11-year solar cycle forcing, *J. Geophys. Res.*, *113*, D22304, doi:10.1029/2008JD010189.

Rosenfield, J. E., A. R. Douglass, and C. B. Considine (2002), The impact of increasing carbon dioxide on ozone recovery, *J. Geophys. Res.*, *107* (D6), 4049, doi:10.1029/2001JD000824.

Rozanov, A., V. V. Rozanov, M. Buchwitz, A. Kokhanovsky, and J. P. Burrows (2005), SCIATRAN 2.0—A new radiative transfer model for geophysical applications in the 175–2400 nm spectral region, *Adv. Space Res.*, *36*, 1015–1019, doi:10.1016/j.asr.2005.03.012.

Rozanov, E., T. Egorova, W. Schmutz, and T. Peter (2006), Simulation of the stratospheric ozone and temperature response to the solar irradiance variability during Sun rotation cycle, *J. Atmos. Sol.-Terr. Phys.*, *68*, 2203–2213, doi:10.1016/j.jastp.2006.09.004.

Ruzmaikin, A., M. L. Santee, M. J. Schwartz, L. Froidevaux, and H. M. Pickett (2007), The 27-day variations in stratospheric ozone and temperature: New MLS data, *Geophys. Res. Lett.*, *34*, L02819, doi:10.1029/2006GL028419.

Sander, S. P., et al. (2005), Chemical kinetics and photochemical data for use in atmospheric studies: Evaluation number 15, *JPL Publ. 06-2*, 523 pp.

Sekiyama, T. T., K. Shibata, M. Deushi, K. Kodera, and J. L. Lean (2006), Stratospheric ozone variation induced by the 11-year solar cycle: Recent 22-year simulation using 3-D chemical transport model with reanalysis data, *Geophys. Res. Lett.*, *33*, L17812, doi:10.1029/2006GL026711.

Skupin, J., M. Weber, S. Noël, H. Bovensmann, and J. P. Burrows (2005), GOME and SCIAMACHY solar measurements: Solar spectral irradiance and Mg II solar activity proxy indicator, *Mem. Soc. Astron. Ital.*, *76*, 1038–1041.

Sonkaew, T., V. V. Rozanov, C. von Savigny, A. Rozanov, H. Bovensmann, and J. P. Burrows (2009), Cloud sensitivity studies for stratospheric and lower mesospheric ozone profile retrievals from measurements of limb scattered solar radiation, *Atmos. Meas. Tech.*, *2*, 653–678.

Soukharev, B. E., and L. L. Hood (2006), Solar cycle variation of stratospheric ozone: Multiple regression analysis of long-term satellite data sets and comparisons with models, *J. Geophys. Res.*, *111*, D20314, doi:10.1029/2006JD007107.

Torrence, C., and G. P. Compo (1998), A practical guide to wavelet analysis, *Bull. Am. Meteorol. Soc.*, *79*, 61–78.

Viereck, R. A., L. E. Floyd, P. C. Crane, T. N. Woods, B. G. Knapp, G. Rottman, M. Weber, L. C. Puga, and M. T. DeLand (2004), A composite Mg II index spanning from 1978 to 2003, *Space Weather*, *2*, S10005, doi:10.1029/2004SW000084.

von Savigny, C., A. Rozanov, H. Bovensmann, K.-U. Eichmann, S. Noël, V. V. Rozanov, M. Weber, J. P. Burrows, and J. W. Kaiser (2005a), The ozone hole breakup in September 2002 as seen by SCIAMACHY on ENVISAT, *J. Atmos. Sci.*, *62*, 721–734.

von Savigny, C., J. W. Kaiser, H. Bovensmann, J. P. Burrows, I. S. McDermid, and T. Leblanc (2005b), Spatial and temporal characterization of SCIAMACHY limb pointing errors during the first three years of the mission, *Atmos. Chem. Phys.*, *5*, 2593–2602.

Weber, M. (1999), Solar activity during solar cycle 23 monitored by GOME, *ESA-WPP-161*, pp. 611–616, Eur. Space Agency, Paris.

Williams, V., J. Austin, and J. D. Haigh (2001), Model simulations of the impact of the 27-day solar rotation period on stratospheric ozone and temperature, *Adv. Space Res.*, *27*(12), 1933–1942.

World Meteorological Organization (2007), Scientific assessment of ozone depletion: 2006, *Global Ozone Res. Monit. Proj. Rep. 50*, 572 pp., Geneva.

Zhou, S., A. J. Miller, and L. L. Hood (2000), A partial correlation analysis of the stratospheric ozone response to 27-day solar UV variations with temperature effects removed, *J. Geophys. Res.*, *105*(D4), 4491–4500.

J. P. Burrows, S. Dikty, A. Rozanov, T. Sonkaew, C. von Savigny, and M. Weber, Institute of Environmental Physics, University of Bremen, Otto-Hahn-Allee 1, D-28359 Bremen, Germany. (dikty@iup.physik.uni-bremen.de)